AD A102760

DTIC FILE COPY

DTIC
ELECTE
AUG 1 2 1981

S

C

Department of Physics and Astronomy

THE UNIVERSITY OF IOWA

Iowa City, Iowa   52242

81 8   12 041

OBSERVATIONS OF HIGH-SPEED PLASMA

FLOW NEAR THE EARTH'S MAGNETOPAUSE:

EVIDENCE FOR RECONNECTION?

by

T. E. Eastman and L. A. Frank

June 1981

The Department of Physics and Astronomy
The University of Iowa
Iowa City, Iowa   52242
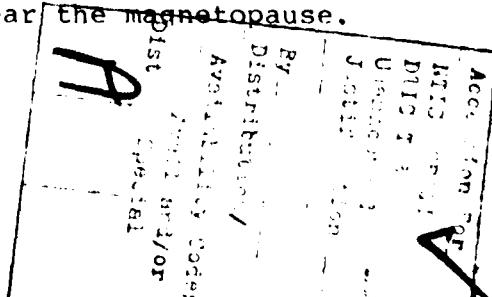
1. Introduction

Since the advent of in situ satellite observations of the earth's magnetopause, investigators have searched diligently for high-speed ion jets, an expected signature of the reconnection process (Vasyliunas, 1975). Significant indirect evidence for the reconnection process has been presented, especially for processes in the magnetotail (Hones et al., 1976; Frank et al., 1976). However, extensive analyses of HEOS 2 (Haerendel et al., 1978) and IMP 6 data (Eastman and Hones, 1979) have failed to reveal any significant high speed ion flow near the magnetopause. These studies demonstrated that the dominant process in the solar wind-magnetosphere interaction results in plasma de-energization as magnetosheath plasma crosses the magnetopause to supply the magnetospheric boundary layer.

ISEE observations have recently provided some potential direct evidence for reconnection via direct measurements of the tangential electric field (Mozer et al., 1979) and high-speed ion flows near the magnetopause (Paschmann et al., 1979). Although the electric field measurements are subject to interpretive problems that are not yet fully resolved, the high-speed plasma flow observations could represent significant evidence for reconnection in the framework of an apparent lack of alternative hypotheses for high-speed flows near the magnetopause.

In this paper, we present ISEE plasma observations using the University of Iowa quadrispherical electrostatic analyzers (LEPEDEAs). These observations supplement those of Paschmann et al. (1979) for the 8 September 1978 (day 251) magnetopause crossing which are based on measurements by the LANL/MPE plasma analyzers. We will present results that relate to the following critical questions for the reconnection hypothesis:

(1) Are the observed flows consistent with those required by the MHD rotational discontinuity conditions?

(2) Are energetic ion and electron signatures observed near the magnetopause consistent with a reconnection geometry?

The presence of a MHD rotational discontinuity is a necessary, although not sufficient, condition for the reconnection mechanism. A further necessary condition is that high-speed plasma flow, produced by the "slingshot" acceleration process of reconnection, must be on open field lines. The energetic electron and ion observation indicate that at least part of the high-speed plasma flow, observed during the 8 September 1978 ISEE magnetopause crossing, is on closed field lines. This magnetopause crossing thus provides an excellent case study in which an observation of high-speed ion flow near the magnetopause does not constitute adequate evidence for the presence of reconnection.

2. Instrumentation

The LEPEDEA instruments sample ion and electron velocity distributions over all except ~ 2% of the unit sphere for particle velocity vectors. These instruments have an energy resolution of $\Delta E/E = 0.16$ and cover an energy range of 1 eV to 45 keV for positive ions and electrons. Depending on instrument mode, 32 or 64 energy passbands are sampled which either span the full energy range or the highest 32 levels which cover energies above 215 eV (e.g., Plates 1 and 2). Polar angles θ measured from the spacecraft spin axis to the individual fields-of-view of the seven detector pairs are illustrated in Figure 1. The spacecraft spin period is approximately 3 sec; 16 azimuthal sectors are sampled at low spacecraft telemetry rate and approximately 12 azimuthal sectors are sampled at high rate. Each instrument cycle used for the full velocity distribution calculation requires 128 sec in the basic high-bit-rate mode (32 energy levels X 4 sec per energy level) and approximately 8 min in the low-bit-rate mode. Instruments were in high-bit-rate mode during the 8 September 1978 magnetopause crossing. With 12 azimuthal sectors and seven polar angles, $12 \times 7 \times 32 = 2688$ samples of velocity space are obtained every 128 sec; at a given energy, seven polar angle are sampled <u>simultaneously</u> each 0.25 sec in successive azimuthal sectors which are separated by approximately 30°. Starting at the lowest energy, each detector (numbered 1-7 as shown in Figure 1) sweeps through all azimuthal (ϕ) angles before stepping up to

the next higher energy level. Corresponding E-ϕ plots are constructed for the seven detector pairs and several examples are presented in Plates 1 and 2. The data frames are labeled 1P-7P in the color plates for detectors 1-7 where "P" denotes protons and "E" denotes electrons. The ions are assumed to be primarily protons for most of the present analysis although a helium ion component is observed and discussed in this paper.

More detailed descriptions of the ISEE LEPEDEA instruments are provided by Frank et al. (1978a, 1978b). Although the LEP-EDEA has a complete cycle time of 128 sec, it covers the full solid angle range during each 3-sec spin period at each energy. The full three-dimensional capability of the LEPEDEA is especially important for the present study in which cool ion distributions with large polar bulk flow components are found. In addition, angular variations of such flows can be detected on a time scale of only a few spin periods. Simultaneous samples with a Geiger-Mueller (GM) tube, which has a collimated 40° field-of-view, provide measurements of the angular distributions of > 45 keV electrons at the midplane of the spacecraft.

In this paper, we employ these capabilities of the quadrispherical LEPEDEA to supplement the information reported previously for the 8 September 1978 ISEE magnetopause crossing. We find that our three-dimensional observations lead to the best available estimates of the flow vector during the high-speed flow interval for this crossing.

3. Observations

a. Energy-Time (E-t) Spectrograms

A color-coded energy-time (E-t) spectrogram is shown in
Plate 1a which covers the first six hours of ISEE-1 measurements
on 8 September 1978 (day 251). The E-t spectrograms display
detector responses coded according to a color scale shown on the
right-hand side of the color plates. Values of $\log_{10}$ (responses)
are shown next to the color bar. The responses are proportional
to the energy, E, multiplied by directional differential energy
flux, dJ/dE, and are proportional to E^2 multiplied by phase space
density, $f(\vec{v})$. The four panels of the spectrograms display, from
top to bottom, averages of responses sampled by the equatorial
plane detector (detector 4) for the sunward-looking quadrant (v),
the duskward-looking quadrant (>), the antisunward-looking quad-
rant (∧) and the dawnward-looking quadrant (<), respectively.
These standard spectrograms also display azimuthally averaged
electron spectra. Values of $\log_{10}$ of the energy in units of eV
are given along the ordinate with time in hours (UT) marked along
the abscissa. Spacecraft coordinates are given in solar ecliptic
coordinates.

As shown in Plate 1a, hot ($\gtrsim$ 10 keV), isotropic ion and
electron distributions are encountered in the outer magnetosphere
until ~ 0040 UT. ISEE-1 plasma parameters from Paschmann et al.
(1979) are reproduced in Figure 2 and include ion number density,
speed and the solar ecliptic z-component of the magnetic field,

B_z. The first magnetopause crossing at 0043:56-59 UT is well
defined in B_z and the high-speed flow region is earthward of
the magnetopause and thus is identified as a magnetospheric
boundary layer. This boundary layer interval is very brief on
the six-hour time scale shown in the E-t spectrogram. The sub-
solar region magnetosheath in this case is highly variable in
density and flow direction based on moments analysis. Large
spectral variations are present in both the sectored ion plots
as well in the azimuthally averaged electron responses shown in
the bottom panel of the E-t spectrogram. Bow shock crossings
are observed at 0327, 0335, 0340, 0405 and 0538 UT.

b. Energy-Phase Angle (E-ϕ) Spectrograms

Three-dimensional response arrays or energy-phase angle
(E-ϕ) plots presented in Plates 1 and 2 cover several instru-
ment cycles for this crossing of the magnetospheric boundary
layer and magnetopause. The time given at the top of each E-ϕ
plot set is the start time for each 128 sec instrument cycle.
Figure 3 illustrates the E-ϕ plot format based on the 6P frame
from Plate 2a. Values of $\log_{10}$ of the proton energy in units
of eV are given along the ordinate. Each frame shows 16 az-
imuthal sector marks on the abscissa. Since the spin axis is
nearly perpendicular to the ecliptic plane, the abscissa may be
interpreted as solar ecliptic longitude of flow direction from
0° (sunward direction) to 360°. Detector responses are dis-
played according to a color-coded scale shown at the right-hand
side of the color plates with appropriate values of $\log_{10}$ of

the responses marked next to the color bar. The 6P frame illus-
trated in Figure 3 shows detector 6 ion responses from the start
time of 0041:41.7 UT to 0043:49.6 UT. Detector 6 views a 21°
polar angle range centered 62° below the ecliptic plane as shown
in Figure 1. These ions are thus flowing upward and tailward.

All frames within the E-φ plots, including the GM frame for
> 45 keV electrons, display responses sequentially from bottom
to top. Thus, energy and time values are isomorphic for 1P-7P
and 1E-7E as shown in Figure 3. Energy channels are logarith-
mically spaced so that the vertical axis is nearly linear in
time. For example, the sharp lower edge for 6P responses occurs
near 0.23 of the full vertical scale which corresponds to a time
of 0.23 X 128 sec after the start time, or 0041:41.7 UT + 29.1
sec = 0042:11 UT. Because detectors 4P-7P all show a rapid
change at this time, the ion distribution changed substantially
in less than one spin period or 3 sec. After that time the dis-
tribution appears relatively stable for at least 30 sec. How-
ever, at later times within this same instrument cycle the LEP-
EDEA is sampling energetic ions above 10 keV until the beginning
of the next instrument cycle at 0043:49.6 UT (Plate 2b). The
response enhancement present in each of the 5E frames is caused
by secondary electrons and photoelectrons that result from the
instrument-satellite configuration.

There are numerous features of the ion and electron velo-
city distributions which can be inferred from the three-
dimensional response arrays. These E-φ spectrograms effectively

provide a direct look at three-dimensional velocity distribu-
tions. In the remainder of this section, we will demonstrate
this capability with a detailed description of the response
arrays shown in Plates 1 and 2.

The nearby outer magnetosphere is dominated by hot (> 10
keV), isotropic ion and electron distributions as shown in Plate
1b after 0038:49 UT (upper third of each frame). In contrast,
low response levels are observed at energies of < 1 keV. From
0038:04 UT to 0038:49 UT, a brief segment of boundary layer plas-
ma is observed which corresponds to results from the LANL/MPE in-
strument at this same time as shown in Figure 2. This boundary
layer segment near 0038:30 UT differs from the later interval
adjacent to the magnetopause near 0044 UT. Later boundary layer
segments do not include a downward flowing component at low ener-
gies whereas this interval shows a significant downward as well
as an upward flowing ion component as shown in Plate 1b, especi-
ally in the 2P, 3P, 6P and 7P frames.

At 0040:35 UT, the E-ϕ spectrogram of Plate 1c shows a rapid
transition from magnetospheric to upward flowing boundary layer
plasma. A simultaneous decrease in energetic electron (> 45 keV)
intensity occurs as shown in the GM frame although pancake-shaped
pitch-angle distributions remain (also see section 3e below).
Downward-flowing ions are no longer present as they were near
0038:30 UT. The moments analysis parameters shown in Figure 2
demonstrate that the boundary layer is present from 0040:35 UT up
to the magnetopause. This is the interval of high-speed ion flow

described by Paschmann et al. (1979); plasma parameters for this time interval will be described in detail in the next section. After the LEPEDEA starts to sample energetic ions above ~ 10 keV, the primary ion population that contributes to the density and velocity moments is not sampled until the next instrument cycle begins at 0041:42 UT. Energetic ions sampled during this high-speed flow event display primarily a pancake-shaped pitch-angle distribution (see section 3e).

Some low-elevation ion flow is shown in Plate 2a between 0041:42 and 0042:12 UT which corresponds to a large drop in flow speed as shown in Figure 2. The flow vector, $\vec{V}$, at this time is directed towards $\phi_{SE} \approx 250°$ and $\theta_{SE} \approx 25°$ which is at ~ 76° with respect to the magnetic field in the spacecraft reference frame. Solar ecliptic longitude is denoted by ϕ_{SE} and θ_{SE} denotes solar ecliptic latitude with $\theta_{SE} = 0°$ in the ecliptic plane and $\phi_{SE} = 0$ directed sunward along the earth-sun line or X_{SE} axis. After 0042:12 UT the flow becomes more field-aligned and the angle between $\vec{V}$ and $\vec{B}$ decreases to 34° for 0042:12 to 0043:08 UT. Although the LEPEDEA can quickly determine the flow direction, the spectra and flow speed from 0041:42 to 0042:12 UT are uncertain. The flow speed estimate obtained by the LANL/MPE instrument drops to ~ 210 km/s at this time which is probably a good estimate due to the low flow elevation angle which brings the flow direction within the $\pm$ 55° polar angle acceptance aperture of that instrument (see section 3c). For the one-minute period after 0042:12 UT, the LEPEDEA samples a fairly stable, high-speed flow which

is most apparent in the 6P and 7P frames. From Figure 1, we see that detectors 6 and 7 sample θ_{SE} values of less than $-51°$. Detailed plasma parameters for this interval are provided in the next section. The energetic ion measurements presented in Plate 2a for the high-speed flow interval show an angular distribution similar to the previous instrument cycle except that detector 7 now has higher response values (see section 3e).

The magnetopause at 0043:56-59 UT (see Plate 2b and Figure 2) is accompanied by termination of the high-speed ion flow and by a sharp drop in ion and electron responses as energies of ~ 400 eV are being sampled. This rapid change is evident in detectors 4 through 7 and occurs in less than one spin period. Most of Plate 2b then shows the E-ϕ spectrogram for the adjacent magnetosheath. An additional E-ϕ spectrogram for the nearby magnetosheath is given in Plate 2d which, similar to Plate 2b, shows a broad magnetosheath ion distribution. High-speed ion flow is present in the intervening time interval of 0046:17-0051:40 UT which includes boundary layer plasma accompanied by frequent, large magnetic field changes.

The simultaneous presence of He^{++} and He^+ ions in the boundary layer during the 8 September 1978 magnetopause crossing has recently been reported by Peterson et al. (1981). The He^+ and He^{++} signatures appear in Plate 2 as dawnward-directed features at energies of 2 to 6 keV in the 4P-7P frames. These signatures are clearly separable in the LEPEDEA E-ϕ spectrograms

from 0042 to 0056 UT as, for example, in the 4P frame of Plate 2c near 4 keV. In the magnetopause and boundary layer near 0049 UT there are two distinct H^+ signatures centered at < 300 eV and ~ 2 keV, respectively. The lower energy H^+ bulk flow in the spacecraft frame is directed toward ϕ_{SE} = 110° and θ_{SE} = 50°, close to the flow direction observed for low-energy H^+ ions in the nearby magnetosheath. In comparison, the more energetic H^+ ions near 2 keV are directed toward ϕ_{SE} = 201° and θ_{SE} = 56° with a speed of ~ 460 km/s. In the combined bulk plasma frame which includes both the low-energy and high-energy H^+ ions, the low-energy ions are flowing about 80° with respect to the magnetic field near 0049 UT. This flow pitch-angle is ~ 50° for the more energetic H^+, He^{++} and He^+ ions sampled near 2 keV, 2.6 keV and 4.3 keV, respectively. In the combined bulk plasma frame, the velocity components ($V_\parallel$) along the magnetic field are 69 km/s, 88 km/s and 64 km/s for the high-energy H^+, He^{++} and He^+ components, respectively.

Plate 2d shows the E-ϕ spectrogram for the LEPEDEA instrument cycle starting at 0052:21 UT in the magnetosheath. The ion velocity distribution sampled here is similar to that sampled in the first magnetosheath interval shown in Plate 2b. In both cases, a higher energy component is present which is superimposed on the main H^+ distribution. These higher energy ions are directed towards ϕ_{SE} = 230° and θ_{SE} = 38° in the spacecraft frame. Three distinct peaks in ion responses are shown on the right side of the 6P frame in Plate 2d at energy values of

approximately 1.5, 3.1 and 5.6 keV. These energy values correspond to the three E/q states of H^+, He^{++} and He^+ with a 1:2:4 ratio assuming the same flow velocity for each species, an assumption which is supported by the above results near 0049 UT. When evaluated in the combined bulk plasma frame, these H^+, He^{++} and He^+ components have $V_{\parallel}$ values of −342 km/s, −352 km/s and −333 km/s, respectively, with flow pitch-angles near 164°. In this same combined bulk plasma frame, the low-energy H^+ component has a flow pitch-angle of 18° and $V_{\parallel}$ = 109 km/s.

If the acceleration process corresponds only to a fixed potential drop so that each species is accelerated to roughly the same kinetic energy, then the speeds for H^+, He^{++} and He^+ should be in the ratio $2:\sqrt{2}:1$. However, the observed speeds are more nearly equal than can be expected from a process involving a fixed potential drop.

Since the He^+/H^+ number density ratio in the solar wind is typically much less than that for He^{++}/H^+, this He^+ is probably of magnetospheric origin. In fact, Peterson et al. (1981) measure a He^+ number density of < 0.003 cm^{-3} for the later magnetosheath interval of 0055-0155 UT. An inspection of Plates 2a-2d indicates that the He^+ and He^{++} components are present throughout the magnetopause and boundary layer. A relatively weak signature of He^+ is also observed in the magnetosheath but only during the first two instrument cycles after 0052 UT.

c.   Ion Flow Analysis

Moments analysis parameters for positive ions for the 8
September 1978 ISEE magnetopause crossing have been given by
Paschmann et al. (1979) and LANL/MPE results for number densi-
ty, temperature and flow speed are reproduced in Figure 2 for
comparison with the complementary LEPEDEA measurements.   For
several sample instrument cycles, horizontal bars on the three
plots shown in Figure 2 present simultaneous LEPEDEA measure-
ments.   Although the temperatures derived from the two instru-
ments are similar, the LEPEDEA density values are systematical-
ly low.   This difference is due to the generally cold ion spec-
tra and the 70-eV low-energy cutoff for the LANL/MPE instrument
whereas the LEPEDEA at this time was operating in a high-energy
mode which covers 215 eV to 45 keV.

The most significant difference in moments analysis re-
sults for this crossing is that for velocity.   Peak ion speeds
measured by the LANL/MPE instrument are lower by more than $\sim$ 90
km/s relative to the peak speed of 582 km/s sampled by the LEP-
EDEA.   The cause of this difference is illustrated in Figure 4.
Polar angle coverage of the seven LEPEDEA detectors is marked
by solid lines emanating from the center of the diagram.   De-
tector 4 is roughly centered on the ecliptic plane since the
spin axis is directed towards ϕ_{SE} = 161.4° and θ_{SE} = 86.6°.
Contours of the ion velocity distribution are drawn about our
observed ion flow vector which is directed 58 $\pm$ 3° above the
ecliptic plane.   Whereas the peak ion response levels are

present in frames 6P and 7P of Plate 2a, the LANL/MPE instrument has a sharp response cutoff at 55° away from the spin plane (Bame et al., 1978) and its 3-D mode effectively covers the range of the LEPEDEA detectors 3 through 5. The effect of this limited angular coverage is to truncate the ion distribution above 55° resulting in a velocity vector centered 45° above the ecliptic plane. Although the LANL/MPE instrument provides reasonable estimates for V_x and V_y, the V_z value is substantially underestimated.

The LEPEDEA obtains approximately seven times more samples of velocity space at this time whereas the LANL/MPE instrument samples the three-dimensional distributions ten times faster. At a given energy, the LEPEDEA has the unique capability of sampling seven pitch angles simultaneously and changes in flow direction can be identified on a time scale of only a few spin periods. As noted in the last section within the description of Plate 2a, a rapid direction change occurs at 0042:12 UT; thereafter, the ion velocity distribution is fairly stable so that the LEPEDEA obtains an adequate sampling of the full three-dimensional velocity distribution. Table 1 below summarizes plasma and field parameters for three time intervals near the magnetopause based on the LEPEDEA and LANL/MPE (Paschmann et al., 1979) plasma instruments and the UCLA flux-gate magnetometer.

Error estimates are obtained for the LEPEDEA values by evaluating both statistical errors and systematic errors associated particularly with in-flight calibration coefficients. Our error

analysis procedure results in approximate rms errors of $\Delta V = 8$ km/s for speed and $\Delta kT = 10$ eV for thermal energy. The boundary layer flow vector is directed $58 \pm 3°$ above the ecliptic plane (compared to ~45° based on the LANL/MPE instrument) and is oriented $34 \pm 2°$ away from the average magnetic field vector.

Table 1. Plasma and Field Parameters for the
8 September 1978 (day 251) ISEE-1 Magnetopause Crossing

Time	(Solar Ecliptic Coordinates) (V_x, V_y, V_z) km/s	$|\vec{V}|$	(B_x, B_y, B_z) nT	ion (cm^{-3})	kT(eV)
0042:12-0043:08 UT	$\dfrac{(-298,-86,493)}{(-290,-82,302)}$	$\dfrac{582}{427}$	$(-25,20,43)$	$\dfrac{5}{9}$	$\dfrac{782}{560}$
~0043:30 UT	(Not Available)		$(-11,24,24)$	18	430
~0044:30 UT	$(-65,24,62)$	93	$(28,34,-33)$	9	193
0048:05-0050:13 UT	$\underline{(-207,-81,280)}$	358	$(-9,25,25)$	15	$\underline{472}$
0052:21-0054:29 UT	$\underline{(-126,-53,133)}$	$\underline{191}$	$(15,45,-17)$	12	215

Note: Underlined values are based on LEPEDEA results (see text).

The tangential stress balance condition for a rotational discontinuity is given by

$$\vec{V}_2 - \vec{V}_1 = (1-\alpha_1)^{1/2} \left(\frac{\rho_1}{4\pi}\right)^{1/2} \left(\frac{\vec{B}_2}{\rho_2} - \frac{\vec{B}_1}{\rho_1}\right) \tag{1}$$

where ρ, $\vec{V}$ and $\vec{B}$ denote the mass density, bulk flow velocity and magnetic field, respectively, on each side of the discontinuity. The pressure anisotropy is defined by $\alpha = 4\pi(P_\parallel - P_\perp)/B^2$ where $P_\parallel$ and $P_\perp$ are the parallel and perpendicular plasma pressures, respectively, (Hudson, 1970). This is a necessary, although not sufficient,

condition for a rotational discontinuity. The application of the MHD discontinuity analysis assumes stationarity and other conditions that cannot be easily checked, if at all. Using the first and third time period given in Table 1, the right-hand side of equation 1 becomes $(1-\alpha_1)^{1/2}$ (386, 102, -553) km/s. This derived $\Delta \vec{V}$ is aligned to within 8° of the observed $\Delta \vec{V}$. However, using the observed pressure anisotropy in the magnetosheath (side 1 of the discontinuity) of -0.14 (Sonnerup et al., 1981), the predicted $|\Delta \vec{V}| = 682$ km/s (G. Paschmann, private communication, 1981) is considerably larger than the observed value of 574 km/s.

A necessary condition for both a tangential and rotational discontinuity is that of pressure balance so that

$$P_{\perp 2} - P_{\perp 1} + (B_2^2 - B_1^2)/8\pi = 0 \qquad (2)$$

where $P_\perp = nkT$ denotes the perpendicular plasma pressure. Total plasma and field pressure is 10.5 ± 0.5 keV/cm^3 in the boundary layer and 9.3 ± 0.4 keV/cm^3 in the nearby magnetosheath. Error estimates arise primarily from the plasma measurements. This pressure imbalance should correspond to a net outward movement of the magnetopause; however, Paschmann et al. (1979) report a net inward magnetopause motion based on timing of magnetic field signatures. This difference suggests that assumptions of the MHD discontinuity analysis are no longer applicable, such as stationarity or the neglect of gradients or finite ion gyroradius effects. A further necessary condition for an MHD rotational discontinuity is

$$V_n = B_n \, ((1-\alpha_1)/\rho)^{1/2}$$

with V_n and B_n designating the normal outward components of bulk
flow velocity and magnetic field, respectively, in the minimum
variance coordinate system. Paschmann et al. (1979) report a val-
ue for B_n of -5.4 ± 2.9 nT. With an average density of 12 cm^{-3}
based on Figure 2 and Table 1, this results in a predicted value
for V_n, in the magnetopause frame, of -20 ± 11 km/s. Our deter-
mination of the angle between the minimum variance normal, n, and
the bulk flow vector for 0042:12 to ~ 0043:08 UT is $88.2 \pm 1.5°$
which corresponds to an observed outward normal flow velocity in
the spacecraft frame of $+18.3 \pm 15$ km/s. Because of the 10 km/s
inward motion of the magnetopause relative to the satellite the
predicted normal plasma velocity, in the spacecraft frame, is -30
km/s (Paschmann et al., 1979). The total angular separation of
the predicted and observed velocity vectors is then approximately
$4.8°$ which is nearly three times our estimated error for project-
ing the bulk flow vector along the minimum variance normal direc-
tion. Paschmann et al. (1979) obtained a negative value for V_n
due to their 55°-truncation of the velocity distribution which re-
duced the measured V_z component as shown in Figure 4. Recently,
Sonnerup et al. (1981) report a slightly modified normal direction
which leads to an observed bulk flow component of $v_n = 8.7$ km/s in
the spacecraft frame and $v_n \simeq 17$ km/s in the magnetopause frame
using a revised magnetopause speed of -8.5 ± 1.5 km/s. An esti-
mate of the average B_n value (-7.2 nT) by Sonnerup et al. (1981)

leads to a predicted $v_n = -55$ km/s, in the magnetopause frame, which corresponds to an even larger angular separation ($7°$) between observed and predicted normal speed components.

Although the V_n value is difficult to estimate directly, we have found that the value for $\cos^{-1}(\frac{\vec{V}}{V}\cdot\vec{n})$ is relatively insensitive to several potential systematic errors or to an extension of the integration time interval to periods prior to 0042:12 UT. This result indicates that the flow vector, even with the flow direction shift near 0042:12 UT, remains closely tangent to the magnetopause surface with $V_n \gtrsim 0$. If the local magnetopause were a tangential discontinuity, then the predicted value for V_n is zero which could be consistent with our results. This situation would also be easier to reconcile with the sharp plasma discontinuity observed coincident with the 2-3 second magnetopause interval, measured by both the LEPEDEA (see Plate 2b) and the LANL/MPE instruments (see Figure 2). Any significant V_n component should be expected to rapidly diffuse away such a sharp plasma gradient.

The total convective electric field, $\vec{E} = -\vec{V} \times \vec{B}$, for the 0042:12-0043:08 UT time interval, has a magnitude of 31 mV/m and is oriented $22°$ with respect to the magnetopause normal. As ISEE-1 approaches the magnetopause, expecially after 0043:30 UT, there is a change in magnetic field orientation that causes $\vec{E}$ to approach the normal direction so that the tangential electric field component, $\vec{E}_t$, is substantially reduced. In the magnetopause frame, the tangential electric field can be written as

$$\vec{E}_t = -(\vec{V}_n \times \vec{B}_t) - (\vec{V}_t \times \vec{B}_n)$$

If we take $V_n \simeq 0$, $V_t = 582$ km/s and $B_n = -5.4$ nT, then $E_t \simeq 3.1$ mV/m (only 10% of the total magnitude) and is nearly parallel to the current vector given in Figure 3 of Paschmann et al. (1979). For $V_n = 20$ km/s, the $-\vec{V}_n \times \vec{B}_t$ term contributes only 1 mV/m so that the $\vec{E}_t$ calculation depends primarily on the B_n value which, in turn, depends on the minimum variance calculation. The minimum variance technique cannot account for changes in magneto- pause orientation during the intervals used to compute B_n; for 8 September 1978, Paschmann et al. (1979) used a six minute inter- val ending at ~ 0045 UT which is about 300 ion gyroperiods. Consequently, the magnetic field observations are consistent with $\vec{E}_t = 0$ at the time of the magnetopause crossing if there are moderate temporal variations in magnetopause orientation.

d.   Characteristics of the Three-Dimensional Ion Velocity
      Distributions

A perspective plot of the three-dimensional ion velocity distribution is shown in Figure 5 based on the 128-sec instrument cycle beginning at 0041:42 UT. This plot covers energy levels from 820 eV to 45 keV; the main peak corresponding to the high- speed plasma flow is based on observations from 0042:12 UT to approximately 0043:08 UT. Energy scans from 215 to 820 eV have been deleted because of a directional shift in the ion distribu- tion near 0042:12 UT. Plasma spectra simultaneously sampled by the LANL/MPE instrument from 0042:12 UT to after 0043 UT show a

low-energy component below 820 eV that has a magnetosheath-like spectrum which is highly variable and reduced in intensity. This magnetosheath-like component is distinct from the high-speed flow component as shown by the three-dimensional response array presented in Plate 2a. If this low-energy component is directly supplied from the magnetosheath, then the plasma injection process filters out ions with small pitch-angles since the nearby magnetosheath ions in this energy range have a much broader angular distribution.

A perspective plot is shown in Figure 6 which is based on observations during the later magnetopause and boundary layer interval. This plasma distribution is very similar to that observed during the earlier high-speed flow period. The nearby magnetosheath distribution is presented as a perspective plot in Figure 7. A peak of high-speed ions directed along $-V_\parallel$ is well separated from the low velocity ion component. Isodensity contours of the ion velocity distributions are presented in Figure 8 for the same three time periods covered by the perspective plots in Figures 5 through 7. These contours show projections of $f(\vec{v})$ onto the $V_\perp$-$V_\parallel$ plane; in each case, the high-speed flow components are well separated from the low-energy ion components. In Figure 8a, an energetic ion peak of moderate intensity is observed near $V_\parallel = +2200$ km/s at low pitch-angles. A comparable high-energy component is also present along $+V_\parallel$ in Figures 5, 7 and 8b; energetic particles will be described further in the next section.

e.   Energetic Ion (10-45 keV) and Energetic Electron (> 45 keV)
      Angular Distributions

The three dimensional response arrays for the boundary lay-
er as presented in Plates 1c, 2a and 2c show energetic ions
above 10 keV. A velocity moments computation was done for 10 to
45 keV ions sampled by the ISEE-1 LEPEDEA. Although the pitch-
angle distributions of energetic ions are peaked at ~ 90° in the
outer magnetosphere, this peak shifts to 109° pitch angle (with
an 84° look azimuth for peak response) and 101° pitch angle
(with a 72° look azimuth for peak response) near 0041:20 UT and
0043:30 UT, respectively, in the boundary layer. Scholer et al.
(1981) present energetic ion data sampled simultaneously by the
NOAA/MPA medium energy particle instrument. Their observations
indicate that an ion anisotropy occurs at these times due to the
loss of ions near an absorbing boundary (Williams, 1979) which
results in significantly decreased energetic ion responses in
the dawnward-looking sectors. Energetic ions with 0-90° pitch-
angles are nearly absent in the 55-65 keV energy range whereas
significant responses are observed in the 45-55 keV energy range
(T. Fritz, private communication, 1981). This trend is consist-
ent with LEPEDEA ion observations near 25 keV which show signi-
ficant responses for pitch-angles < 22° without any comparable
ions directed along $-V_\parallel$ (see plates 2a and 2c and Figures 5, 7, 8a
and 8b). An energy-dependent process is thus involved which
selectively removes 0-90° pitch angle ions out of an otherwise
pancake-shaped pitch-angle distribution; this process also affect-

higher energy ions ($\gtrsim$ 45 keV) more than ions in the 10-45 keV energy range.

Angular distributions of energetic electrons ($\gtrsim$ 45 keV) are sampled with a GM tube in the LEPEDEA instrument. This detector has a 40° conical field-of-view and is described further in Frank et al. (1978a, 1978b). Azimuthally averaged energetic electron intensities from ISEE-1 are plotted in Figure 9. Pancake-shaped pitch-angle distributions are present throughout the boundary layer and outer magnetosphere, as shown by pitch-angle plots presented in the upper right-hand portion of Figure 9 for selected times marked on the azimuthally averaged intensity-vs-time plot. Even during the local intensity decreases near 0038 and 0042 UT, this pitch-angle signature is retained.

Since the energetic electrons have large guiding center speeds ($\sim$ 10 R_E/s at 50 keV for α = 60°) their angular distributions and intensities quickly reflect changes in large-scale field topology. In comparison, the ion flow speed and the Alfvén speed are lower by factors of > 100. If the boundary layer were on open field lines as required in a reconnection model, then energetic electrons within the high-speed flow region should rapidly develop asymmetric, field-aligned distributions such as that observed in the magnetosheath near 0044:30 UT. Two observations in particular indicate that the boundary layer observed during this crossing is on closed field lines:

(1) Pancake-shaped energetic electron pitch-angle dis-
tributions are observed for the entire boundary layer
interval,

(2) A rapid intensity decrease occurs at the magneto-
pause.

The latter observation is not consistent with a significant
local B_n component which would provide for rapid leakage of
energetic electrons across the magnetopause. If an intense and
unusually prolonged energetic electron source was present
equatorward of the ISEE satellites, then the observed symmetric
angular distributions could possibly be produced. However, if
this source occurs on open field lines, as would be the case in
a diffusion region for merging, then there should be signifi-
cant intensity levels of energetic electrons in the adjacent
magnetosheath. Near 0045:20 UT, the energetic electrons in the
magnetosheath have a pitch-angle distribution peaked near 90°.
However this condition is only very briefly observed, occurs
close to the magnetopause intensity gradient and occurs with
low responses so that this anisotropy is compatible with a
brief excursion into the adjacent magnetosheath. For example,
there could be a compression of magnetosheath flux tubes
against the frontside magnetopause resulting in brief intervals
of pseudo-trapping of energetic particles between high field
regions. However, such pseudo-trapping will be weak due to the
large loss cone.

The energetic particle observations provide a valuable supplement to the analysis of a magnetopause crossing. For the high-speed flow interval observed during the 8 September 1978 ISEE crossing we note that (1) the energetic ions have a generally pancake-shaped pitch-angle distribution which shows an azimuthal anisotropy due to the loss of ions from finite ion-gyroradius effects near an absorbing boundary, (2) some energetic ions are present at low pitch-angles ($< 25°$), and (3) pancake-shaped energetic electron distributions are present throughout the boundary layer. These observations indicate that the boundary layer is situated primarily, if not entirely, on closed field lines.

4. Conclusions

In this paper we have endeavored to confirm the evidence for reconnection reported by Paschmann et al. (1979) based on an ISEE satellite traversal of the sunward magnetopause near local noon on 8 September 1978. We have made a detailed analysis of three-dimensional plasma velocity distributions obtained with the University of Iowa LEPEDEA instruments. The observations described include ions and electrons from 215 eV to 45 keV as well as energetic electrons > 45 keV.

The reconnection geometry suggested for this crossing by Paschmann et al. (1979) is shown in Figure 10. Since the observed plasma flow and boundary layer location are asymmetric with respect to the magnetopause, an asymmetric reconnection model, such as that used by Paschmann et al. (1979), is a reasonable hypothesis. However, there are significant differences between observed and predicted plasma parameters - e.g., compare Figure 2 in this paper with Figure 3 in Yang and Sonnerup (1977). The reconnection geometry requires the high-speed boundary layer flow to occur on open field lines. Energetic electron (> 45 keV) pitch-angle distributions sampled by the LEPEDEA, however, show a pancake-shaped distribution with intensities peaked near 90° pitch angle. As we approach the diffusion region or x-line within a reconnection geometry, the field magnitude decreases whereas a magnetic mirror for energetic electrons requires a substantial field increase. If the high-speed plasma flow is on open field lines, then the energetic electrons will be very rapidly lost

with a time scale on the order of their bounce time (~ 1.5 sec)
and no electrons should be observed returning from the diffusion
region. On the contrary, significant energetic electron inten-
sity levels are present during the high-speed flow interval as
shown in Figure 9. Furthermore, their intensity rapidly de-
creases near the magnetopause as expected for a transition from
closed to open field lines. If we introduce particle mirrors in
the magnetosheath or strong and steady sources of energetic par-
ticles in the diffusion region or along the magnetopause, then
the steep intensity gradient at the magnetopause cannot be ac-
counted for. If sufficient and thus strong pitch-angle scatter-
ing is introduced to maintain pancake-shaped energetic particle
distributions on open field lines, the low magnetosheath inten-
sity level is still a problem since energetic electrons will be
scattered into the 90-180° pitch-angle range and subsequently
lost due to large loss-cone angles even in the presence of flux
tube compression against the frontside magnetopause.

At the magnetopause near 0044 UT, within one spin period (3
sec), the ISEE-1 LEPEDEA instrument observes a sharp decrease in
ion intensity concurrent with the primary change in B_z. In add-
ition to the correspondingly steep gradient in > 45 keV energet-
ic electron intensity based on the LEPEDEA GM data, the LANL/MPE
ion and electron responses and the NOAA/MPA measurements of 30-
60 keV electrons also show a simultaneous sharp decrease at the
magnetopause. Based on a 10 km/s inward magnetopause motion,
the $\sim$ 3 sec magnetopause transition corresponds to a nominal

30 km magnetopause thickness. If the predicted v_n values of -20 km/s (Paschmann et al., 1979) or -55 km/s (Sonnerup et al., 1981) apply to this magnetopause transition, then the particle gradient at the magnetopause should be spread out to a thickness of 3 sec X 20 km/s = 60 km or 3 sec X 55 km/s = 165 km, respectively, even if the finite normal flow was initiated at the same time as the magnetopause crossing. Noting also that the gyroradius is 85 km for 2 keV ions with a 1.2 sec gyroperiod, this magnetopause does not appear to be further broadened by a finite v_n value. We note that Paschmann et al. (1979) identified a magnetopause interval of 90 sec and used a six-minute interval of magnetic field data to complete the minimum variance analysis. However, based on the 1/16 sec resolution field data, the primary change in field magnitude and especially B_z is limited to 0043:56-59 UT which we take as the primary current layer, or magnetopause layer. Paschmann et al. (1979) obtained v_n values that were predominantly negative due to their 55°-truncation of the velocity distribution. With a full sampling of the ion velocity distributions over the 0042:12-0043:08 UT time intervals, we found V_n to be +17 or +27 km/s, in the magnetopause frame, depending on the normal direction used. If we assume that V_n was actually zero at this time, then it could have become negative by the time that ISEE-1 crossed the magnetopause near 0044 UT. This condition, however, is difficult to reconcile with the steep particle and field gradients observed at the magnetopause.

Since helium ions are accelerated to a speed comparable to that of the high-speed H^+ component instead of gaining a comparable energy, a process which predicts a uniform velocity increase should be preferred to a process which involves a uniform energy transfer. For acceleration from a magnetic slingshot with $\vec{E} = -\vec{V} \times \vec{B}$, different ions will be accelerated by the same velocity increments whereas, for acceleration close to the diffusion region where $\vec{V} \times \vec{B}$ can be small compared to the reconnection electric field, ion acceleration will occur at the same energy increments.

Regarding the uniqueness of the reconnection hypothesis for the 8 September 1978 ISEE observations, D'Angelo (1979) has proposed an alternative model. His Laval nozzle model predicts a uniform velocity increase comparable to the observed values and also considers the high speed flow to be on closed field lines. For an ion sound speed of $V_S = 188$ km/s and a typical range of values for $M = V/V_S$ of 3 to 3.3 (D'Angelo, 1979), where M is the flow Mach number, the predicted flow speeds that result from the Laval nozzle model are 560-620 km/s. Consequently, the observed high flow speeds observed in the boundary layer cannot be considered as uniquely predicted by the reconnection model. At this stage of development, however, it is not clear how applicable the Laval nozzle model is to the ISEE observations discussed in this paper.

Our analysis has led to the following results which could be taken as supportive of the reconnection hypothesis:

1) High-speed ion flow occurs within the boundary layer and reaches a speed of 582 km/s which is close to the Alfvén speed based on the difference magnetic field (Paschmann et al., 1979).

2) The tangential stress balance condition (equation 1, previous section) is roughly met. This condition is one of the necessary conditions for a MHD rotational discontinuity which, in turn, is a necessary condition for the reconnection geometry. Since this condition is derived directly from Maxwell's equations and the energy momentum tensor, any process such as nonlinear plasma turbulence which results in a locally finite average B_n value will satisfy the tangential stress balance condition.

At this juncture, we can only conclude that some of the conditions for a MHD rotational discontinuity are met based on local satellite observations. Since reconnection is a process which involves global topological conditions (Vasyliunas, 1975), our results cannot be considered as meeting sufficient conditions for the presence of reconnection. A further difficulty concerns the general applicability of a MHD "fluid" description to the magnetopause interaction region with its large spatial and temporal variations involving a medium-β plasma where kinetic instabilities are probably important (Gary and Eastman, 1979).

We find that available observational results for the 8 September 1978 magnetopause crossing lead to several difficulties for the reconnection interpretation:

1) Observed high-speed flow events are at least partly on closed field lines and, perhaps, partly on open field lines (Scholer et al., 1981).

2) Energetic ions and electrons, sampled during the high-speed plasma flow interval, show no large decrease in intensity upon crossing into the region of reconnected field lines.

3) The reconnected "flux tube" is not emptied of energetic particles for > 160 sec although the bounce time for $60°$ pitch-angle particles is $\sim$ 80 sec and $\sim$ 1.5 sec, respectively, for these ions and electrons.

4) If energetic particles are supplied by a source in a diffusion region for reconnection, this source supplies low energy plasma sporadically although it continuously and uniformly supplies energetic particles.

5) Observed energetic particles and low energy plasmas have a steep gradient at the magnetopause which is difficult to reconcile with a finite B_n value.

6) The observed value for v_n is not consistent with the predicted value without introducing rapid temporal variations in magnetopause orientation. However, such magnetopause variations would tend to invalidate the minimum variance analysis.

The combined results of this paper place a number of con-
straints on any model used to explain signatures of the 8 Sep-
tember 1978 ISEE magnetopause crossing. Although this crossing
shows high-speed ion flow in the boundary layer, the energetic
pitch-angle distributions indicate that this high-speed flow
occurs partly or entirely on closed field lines. For a recon-
nection model, the high-speed flow should occur only on open
field lines; this prediction applies as well to "patchy" recon-
nection models. Thus, to consistently apply the reconnection
interpretation, a second mechanism must be introduced to explain
the high-speed flow observed on closed field lines unless rapid
diffusion occurs onto the closed field line region. Such rapid
diffusion, however, is not entirely consistent with the observed
density and flow speed profiles and could equally well be used
to supply the boundary layer without reconnection.

Given the difficulties in placing all, or even part of,
the high speed plasma flow on open field lines, we will now
consider whether the observations are consistent with a bound-
ary layer located entirely on closed field lines. Figure 11
illustrates a possible boundary geometry for the 8 September
1978 ISEE magnetopause crossing. The intersections of boundary
lines with the ISEE-1 and -2 trajectories fit the available
plasma observations. The distance from the magnetopause to the
satellites at other times is drawn to be consistent with the
energetic ion observations based on the sounding technique of
Williams (1979). In addition to explaining the trapped-like

energetic particle signatures observed earthward of the magnet-
opause, this picture can account for observed asymmetries of
the ion pitch-angle distributions. Energetic ions with gyro-
diameters that intersect the magnetopause will be lost from the
ion distribution for dawnward-looking azimuths. The loss of
60-90° pitch angles from the energetic ion distributions (Scho-
ler et al, 1981) is enhanced at higher energies due to larger
ion gyroradii; an energy-dependent process that also results in
the absence of upward-flowing, low pitch-angle > 45-keV ions.
At lower energies, the low pitch-angle component comprises ions
which have mirrored without being subsequently lost at the ab-
sorbing boundary. The enhanced loss of ions at 60-90° pitch-
angles is likely due to the increased path length for these
ions close to an absorbing boundary whereas ions returning from
the northern hemisphere are less likely to be lost at the mag-
netopause due to their reduced path length close to an absorb-
ing boundary. This process provides a simple explanation for
the energetic ion distributions that start out peaked from 60-
120° in the inner boundary layer and then lose the < 90° por-
tion close to the magnetopause (Scholer et al., 1981). Inten-
sity variations of energetic particles in the boundary layer
can be accounted for by variable magnetopause positions and
geometry.

Based on these various considerations, we conclude that
the high-speed flow observed in the boundary layer during this

crossing may be the result of impulsive injection of magneto-sheath plasma across the magnetopause (Lemaire, 1977). The conditions for such impulsive entry were enhanced by the highly variable magnetosheath flow and a strong southward field component (Lemaire et al., 1978). Since there is a significant cross-field flow component for the plasma jet which is located on closed field lines, this plasma will soon lose its momentum via local dissipation and closure currents through non-local dissipative regions such as the cusp ionosphere. The cross-field ion flow will thus contribute to the MHD dynamo process that drives the dayside high-latitude current system (Eastman et al., 1976). Our results still leave the entry process un-specified; however, MHD and plasma kinetic instabilities are probably very important and should be a principal focus for theoretical efforts directed toward the magnetopause inter-action problem.

Acknowledgments

References

Bame, S. J., J. R. Asbridge, H. E. Felthauser, J. P. Glore, G. Paschmann, P. Hemmerich, K. Lehmann, and H. Rosenbauer, ISEE 1 and 2 fast plasma experiment and the ISEE 1 solar wind experiment, IEEE Trans. Geosci. Electr., GE-16, 216, 1978.

D'Angelo, N., On "Plasma acceleration at the earth's magneto-pause: Evidence for reconnection", U. of Iowa preprint 79-50, 1979.

Eastman, T. E., E. W. Hones, Jr., S. J. Bame, and J. R. Asbridge, The magnetospheric boundary layer: Site of plasma, momentum and energy transfer from the magneto-sheath into the magnetosphere, Geophys. Res. Lett., 3, 685, 1976.

Eastman, T. E., and E. W. Hones, Jr., Characteristics of the magnetospheric boundary layer and magnetopause layer as observed by IMP 6, J. Geophys. Res., 84, 2019, 1979.

Frank, L. A., K. L. Ackerson and R. P. Lepping, On hot tenuous plasmas, fireballs, and boundary layers in the earth's magnetotail, J. Geophys. Res., 81, 5859, 1976.

Frank, L. A., D. M. Yeager, H. D. Owens, K. L. Ackerson and M. R. English, Quadrispherical LEPEDEDEAs for ISEE 1 and 2 plasma measurements, IEEE Trans. Geosci. Electr., GE-16, 221, 1978a.

Frank, L. A., K. L. Ackerson, R. J. DeCoster and B. G. Burek,
Three-dimensional plasma measurements within the earth's
magnetosphere, Space Sci. Rev., 22, 739, 1978b.

Gary, S. P., and T. E. Eastman, The lower hybrid drift insta-
bility at the magnetopause, J. Geophys. Res., 84, 7378,
1979.

Haerendel, G., G. Paschmann, N. Sckopke, H. Rosenbauer, and P.
C. Hedgecock, The frontside boundary layer of the magneto-
sphere and the problem of reconnection, J. Geophys. Res.,
83, 3195, 1978.

Hones, E. W., Jr., S. J. Bame, and J. R. Asbridge, Proton flow
measurements in the magnetotail plasma sheet made with IMP
6, J. Geophys. Res., 81, 227, 1976.

Hudson, P. D., Discontinuities in an anisotropic plasma and
their identification in the solar wind, Planet. Space
Sci., 18, 1611, 1970.

Lemaire, J., Impulsive penetration of filamentary plasma ele-
ments into the magnetospheres of the earth and Jupiter,
Planet. Space Sci., 25, 887, 1977.

Lemaire, J., M. J. Rycroft, and M. Roth, Control of impulsive
penetration of solar wind irregularites into the magneto-
sphere by the interplanetary magnetic field direction,
Aeronomica Acta, No. 193, Belgian Space Aeronomy Insti-
tute, 1978.

Mozer, F. S., R. B. Torbert, U. V. Fahleson, C.-G. Falthammer, A. Gonfalone, A. Pederson, and C. T. Russell, Direct observation of a tangential electric field at the magnetopause, Geophys. Res. Lett., 6, 305, 1979.

Paschmann, G., B.U.Ö. Sonnerup, I. Papamastorakis, N. Sckopke, G. Haerendel, S. J. Bame, J. R. Asbridge, J. T. Gosling, C. T. Russell, and R. C. Elphic, Plasma acceleration at the earth's magnetopause: Evidence for reconnection, Nature, 282, 243, 1979.

Peterson, W. K., E. G. Shelley, G. Haerendel, and G. Paschmann, Energetic ion composition in and near the subsolar magnetospheric boundary layer, to be submitted to J. Geophys. Res., 1981.

Scholer, M., G. Paschmann, P. W. Daly, T. E. Eastman, T. A. Fritz, and G. K. Parks, Energetic particle signatures during a possible magnetopause reconnection event, to be submitted to J. Geophys. Res., 1981.

Sonnerup, B.U.Ö, G. Paschmann, I. Papamastorakis, N. Schopke, G. Haerendel, S. J. Bame, J. R. Asbridge, J. T. Gosling, and C. T. Russell, Evidence for magnetic field reconnection at the earth's magnetopause, submitted to J. Geophys. Res., 1981.

Williams, D. J., Magnetopause characteristics inferred from three-dimensional energetic particle distributions, J. Geophys. Res., 84, 101, 1979.

Yang, C.-K., and B.U.Ö. Sonnerup, Compressible magnetopause reconnection, J. Geophys. Res., 82, 699, 1977.

Plate Captions

Plate 1.   A.   E-t spectrogram of ISEE-1 LEPEDEA

responses for 8 September 1978, day 251

B.   E-ϕ spectrogram for 251/78 from 0037:26

to 0039:34 UT

C.   E-ϕ spectrogram for 251/78 from 0039:34

to 0041:42 UT

Plate 2.   A.   E-ϕ spectrogram for 251/78 from 0041:42

to 0043:50 UT

B.   E-ϕ spectrogram for 251/78 from 0043:50

to 0045:58 UT

C.   E-ϕ spectrogram for 251/78 from 0048:05

to 0050:13 UT

D.   E-ϕ spectrogram for 251/78 from 0052:21

to 0054:29 UT

Plate 1 will be published in color

Plate 2 will be published in color

Figure Captions

Figure 1.   Instrument fields-of-view for the quadri-
spherical electrostatic analyzers or
LEPEDEAs (from Frank et al., 1978a).

Figure 2.   Plasma and magnetic field data for the
ISEE-1 magnetopause crossing of 8 September
1978. Satellite coordinates are given in
the geocentric solar magnetospheric, GSM,
system. Plasma data presented as solid
lines are from the LANL/MPE instrument
(Paschmann et al., 1979). Simultaneous LEP-
EDEA measurements are marked by a "⊢⊣" sym-
bol. The first magnetopause crossing is
shown by a dashed vertical line near 0044
UT.

Figure 3.   Illustration of the E-ϕ plot format. All
seven detector pairs sample from low-to-high
energy values over the instrument cycle time
which is 128 sec in high-bit-rate mode.
Both energy and time are marked along the
ordinate. The abscissa shows the solar
ecliptic longitude of flow direction.

Figure 4.   Viewing geometry for the ISEE plasma instru-
             ments for the 8 September 1978 magnetopause
             crossing. Polar angle ranges-of-view for
             the seven LEPEDEA detector pairs are shown.
             Approximate phase-space density contours are
             shown for the high-speed boundary layer
             plasma flow. The $\pm$ 55° elevation angle cut-
             off for the LANL/MPE instruments is shown
             along with the flow vector that results from
             this truncated sampling of the ion velocity
             distribution.

Figure 5.   Perspective plot of the three-dimensional
             ion velocity distribution in the boundary
             layer sampled by the ISEE-1 LEPEDEA on 8
             September 1978 from 0041:42 to 0043:50 UT.
             The high-speed flow peak is located at a
             pitch-angle of 34° and has a bulk flow speed
             of 482 km/s.

Figure 6.   Perspective plot of the three-dimensional
             ion velocity distribution in the magneto-
             sheath sampled by the ISEE-1 LEPEDEA on 8
             September 1978 from 0052:21 to 0054:29 UT.

Figure 7.   Perspective plot of the three-dimensional
             ion velocity distribution in the magneto-
             pause and boundary layer interval sampled by
             the ISEE-1 LEPEDEA on 8 September 1978 from
             0048:05 to 0050:13 UT.

Figure 8.   Isodensity contours of three rest-frame ion
             distribution functions based on observations
             by the ISEE-1 LEPEDEA on 8 September 1978.
             These three plots correspond to Figures 5, 7
             and 6, respectively, for distributions sam-
             pled in (a) the boundary layer, (b) the
             later magnetopause and boundary layer inter-
             val and (c) the magnetosheath.
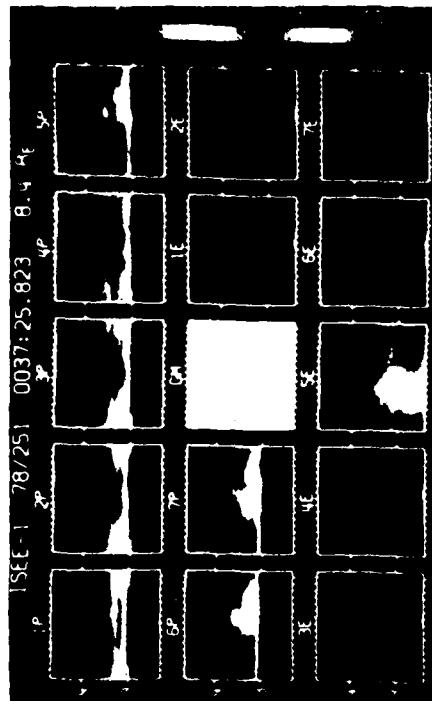
Figure 9.   Energetic electron (> 45 keV) average inten-
             sities and pitch-angle distributions sampled
             with the ISEE-1 LEPEDEA's Geiger-Mueller
             tubes. These measurements span the period
             0037 to 0057 UT on 8 September 1978. Pitch-
             angle distributions are given at upper right
             for each numbered period.
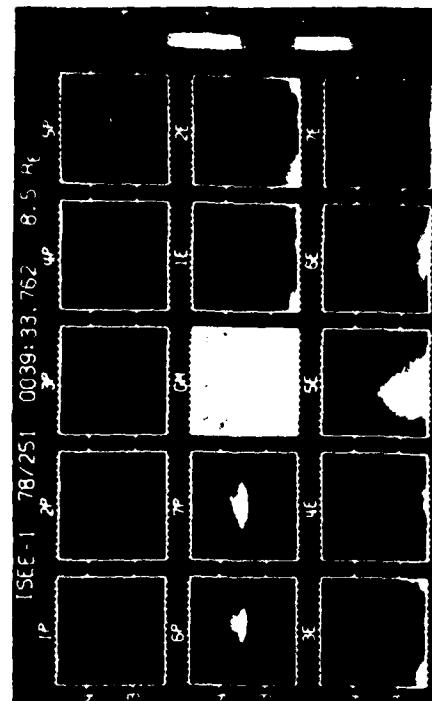
Figure 10.   Boundary and field geometry for the recon-
nection hypothesis as applied to the 8 Sep-
tember 1978 magnetopause crossing (from
Paschmann et al., 1979). The shaded area
denotes the boundary layer, considered to be
on open field lines, and the dashed line
identifies the magnetopause.
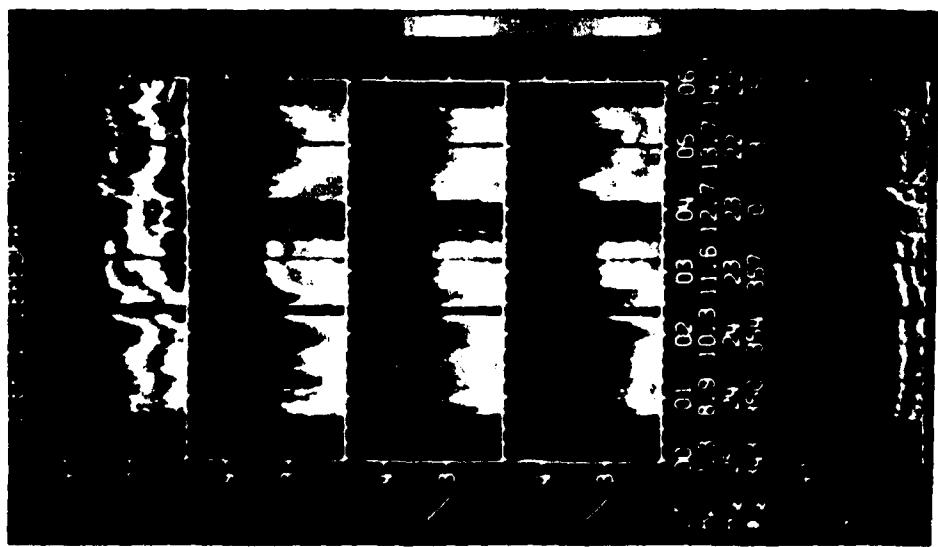
Figure 11.   Boundary layer and magnetopause geometry for
the 8 September 1978 ISEE crossing based on
all available plasma and field data. Brief
intervals of reduced energetic electron
intensity near 0038 and 0042 UT (see Figure
9) could possibly be on open field lines;
however, this diagram illustrates a simple
hypothesis for which the boundary layer is
placed entirely on closed field lines (see
text).

43

B

C

A

Plate 1

44

Plate 2

A-G80-630-1

LEPEDEA FIELDS-OF-VIEW
SPACECRAFT COORDINATES

Figure 1

ISEE-1 MAGNETOPAUSE CROSSING 8 SEPT. 1978 (DAY 251)
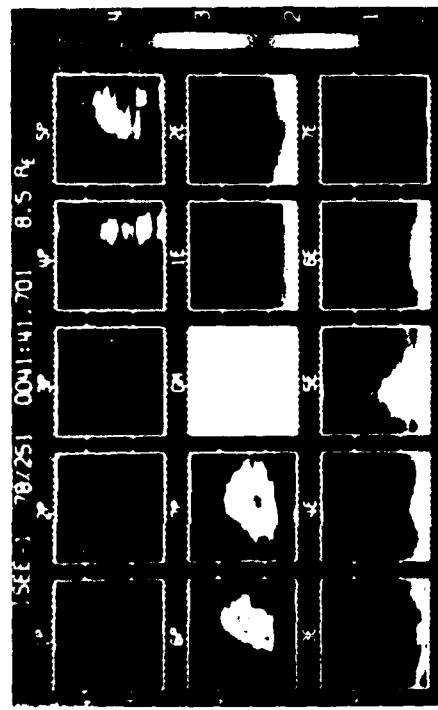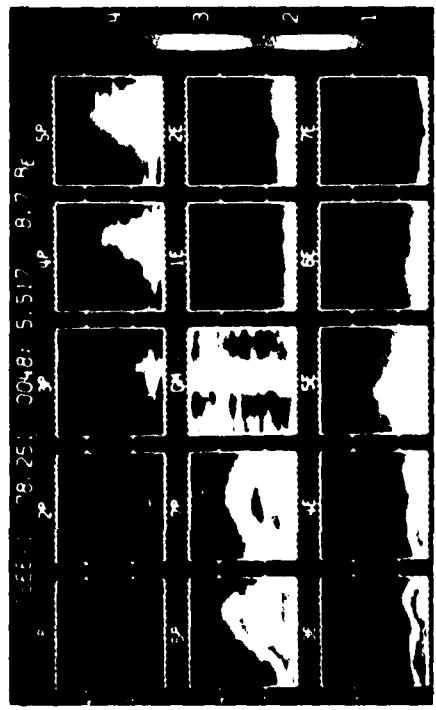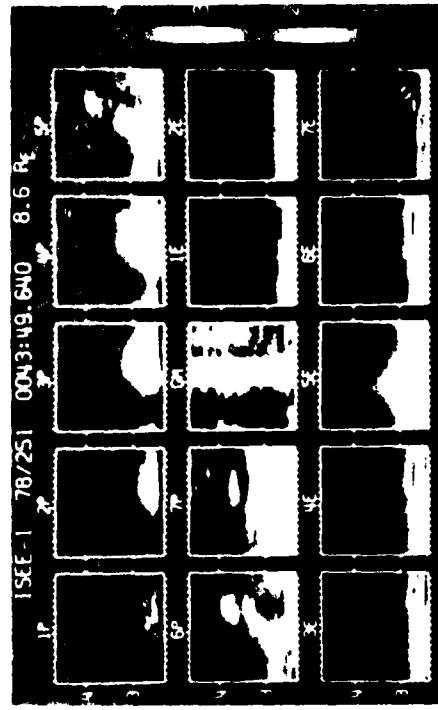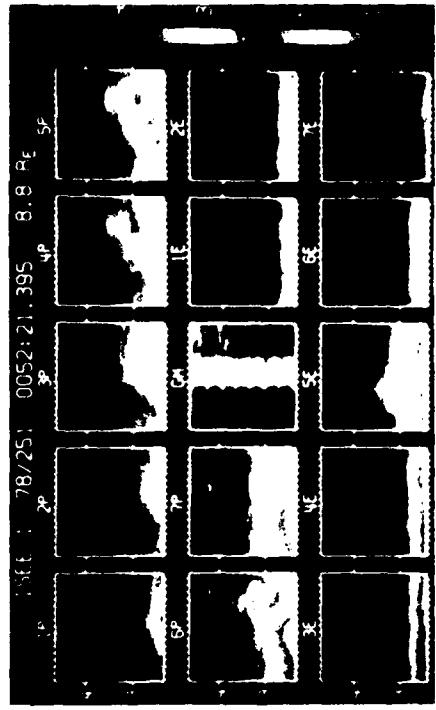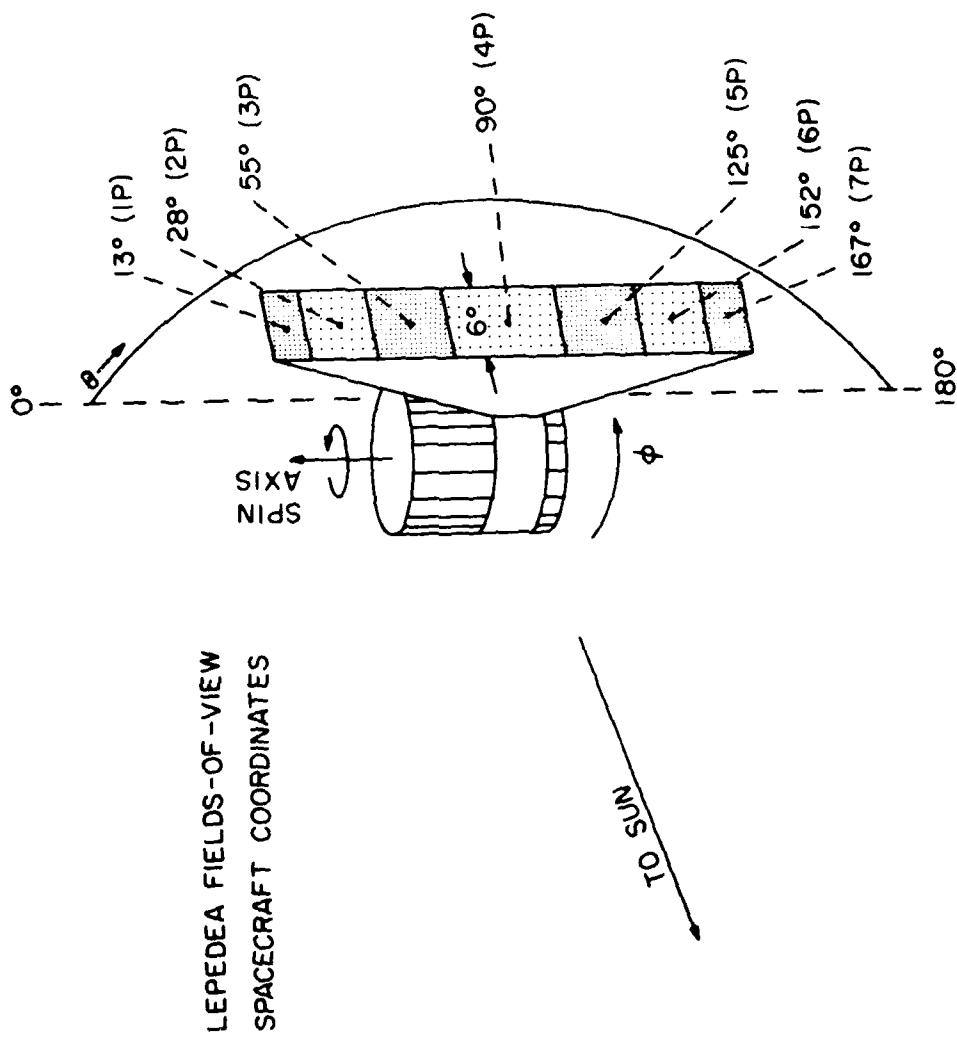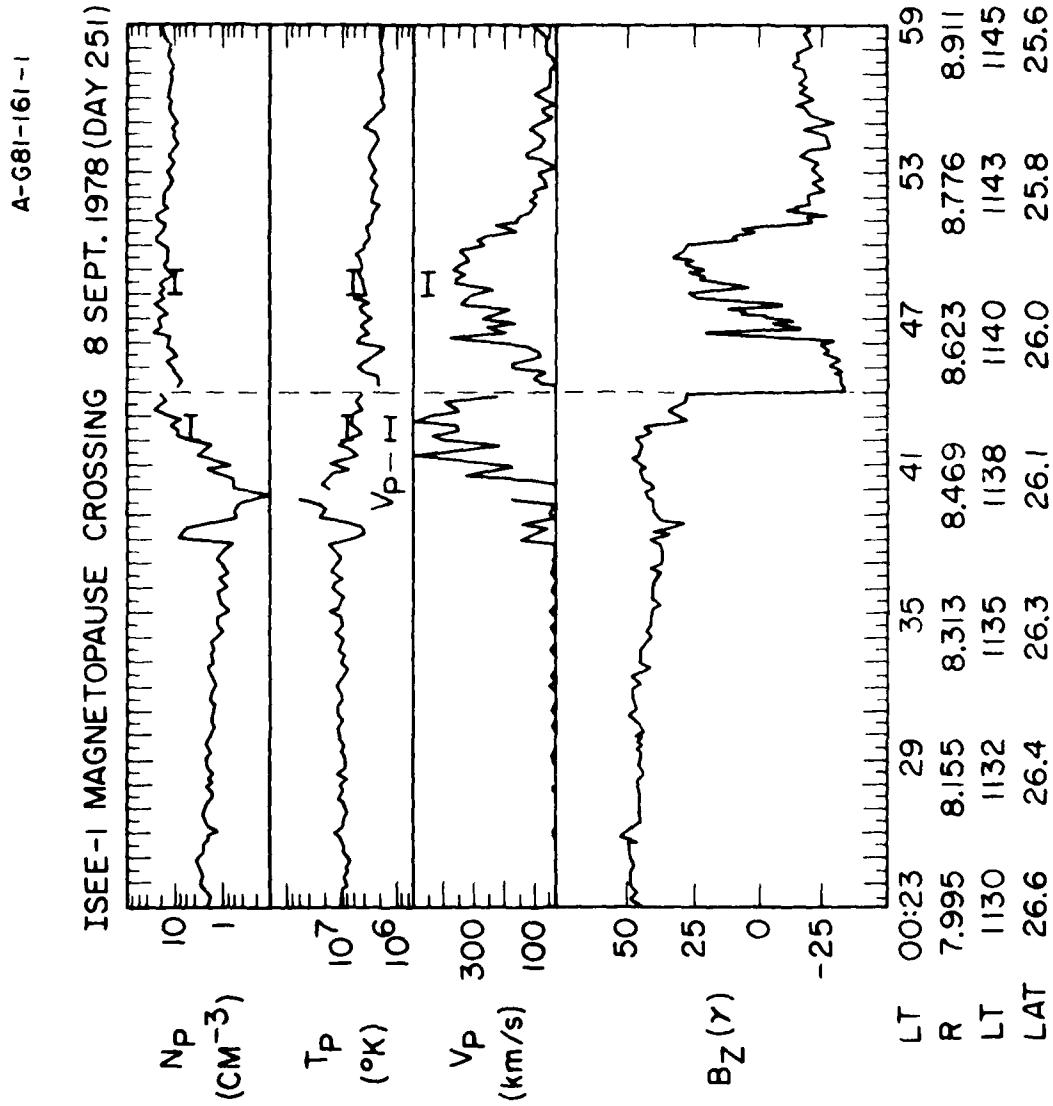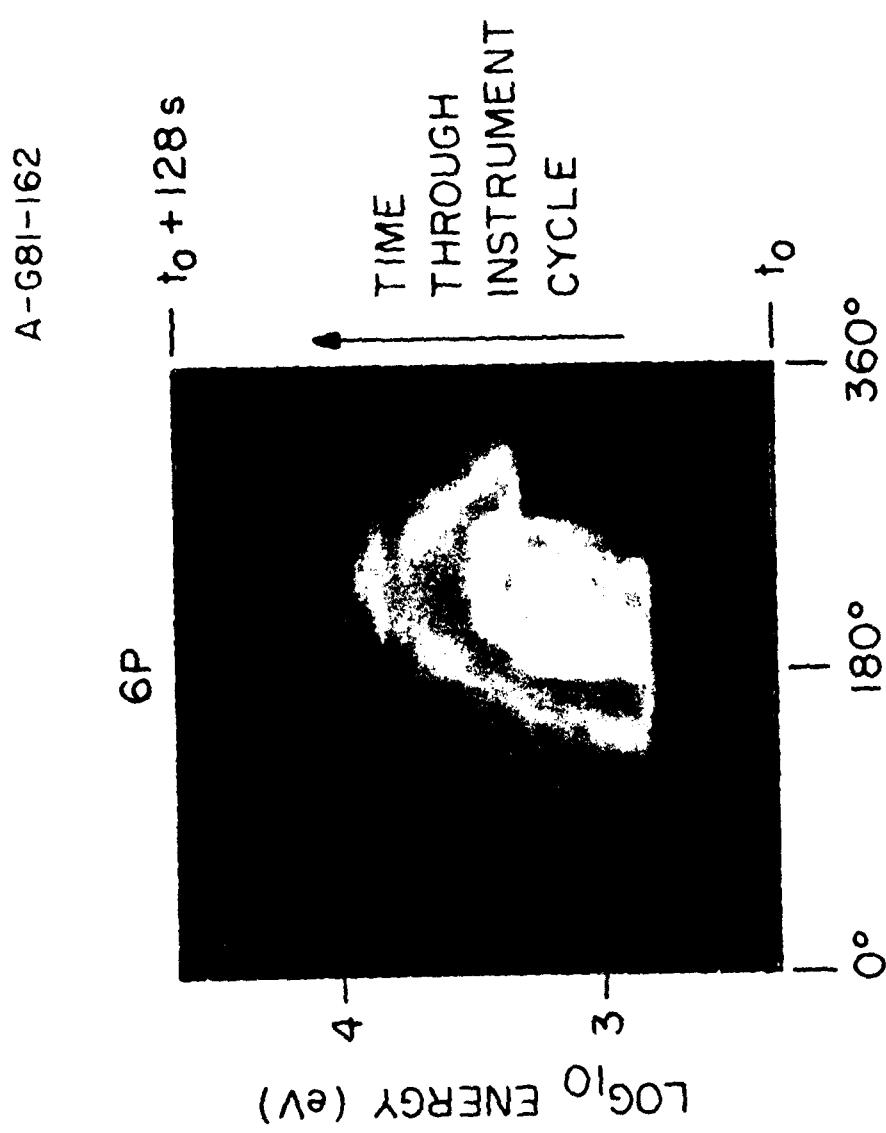
Figure 2

Figure 3

A-G80-732-1

VIEWING GEOMETRY
FOR ISEE PLASMA INSTRUMENTS
MAGNETOPAUSE CROSSING, 251/78

Figure 4

A-G8I-428

ISEE - 1
8 SEPTEMBER 1978
0041:42 - 0043:50 UT

$V_{||}$

$f(V)$

$V_\perp$

30×10^2

20

0

-10

-20

-30

30×10^2
KM/S

20

0

10^{-22}

10^{-24}

10^{-26}

10^{-28}

$f(V)$, CM^{-6} S^3

Figure 5

A-G81-430
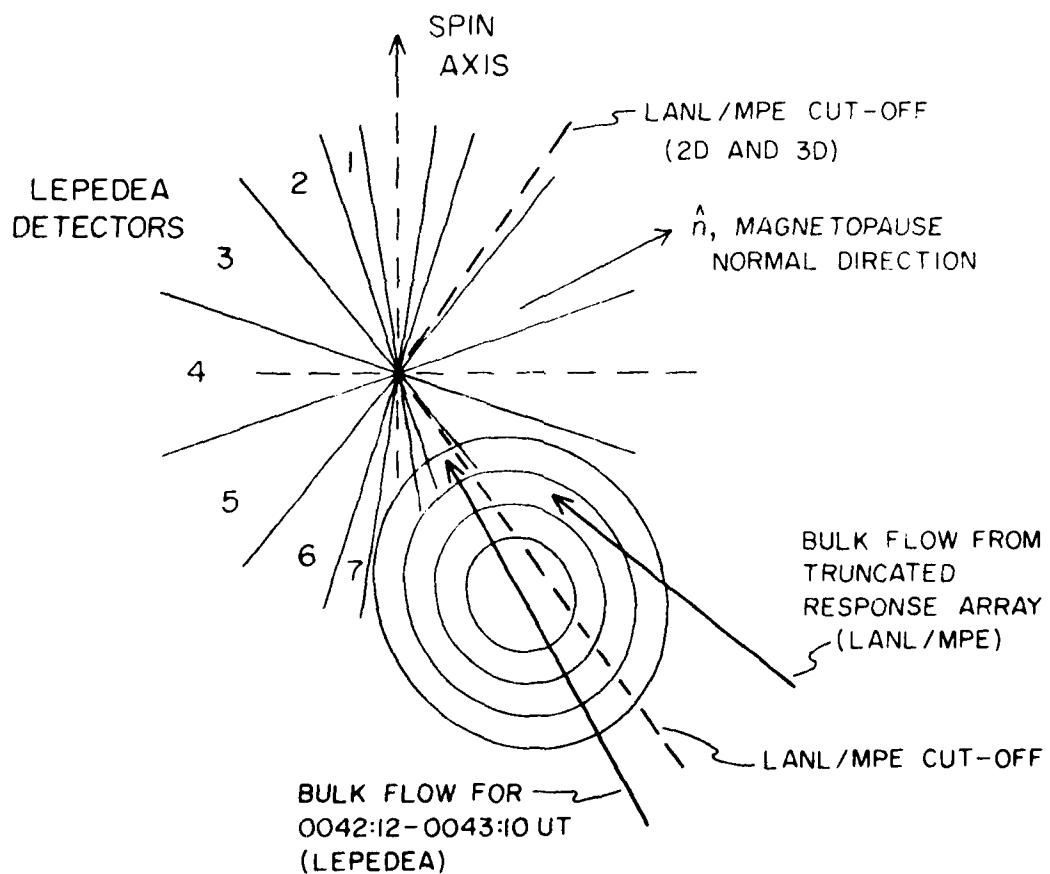
ISEE-1
8 SEPTEMBER 1978
0052:21-0054:29 UT
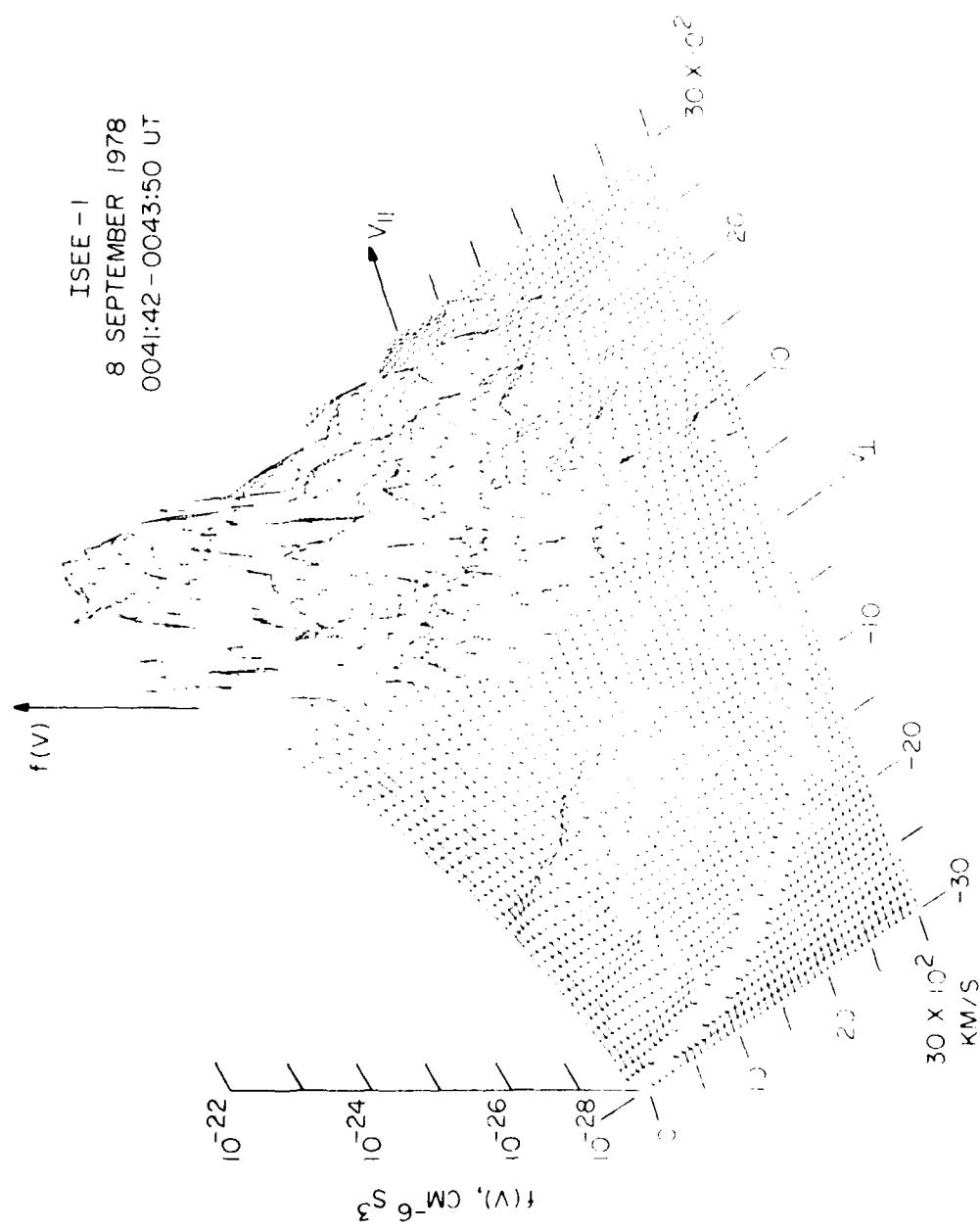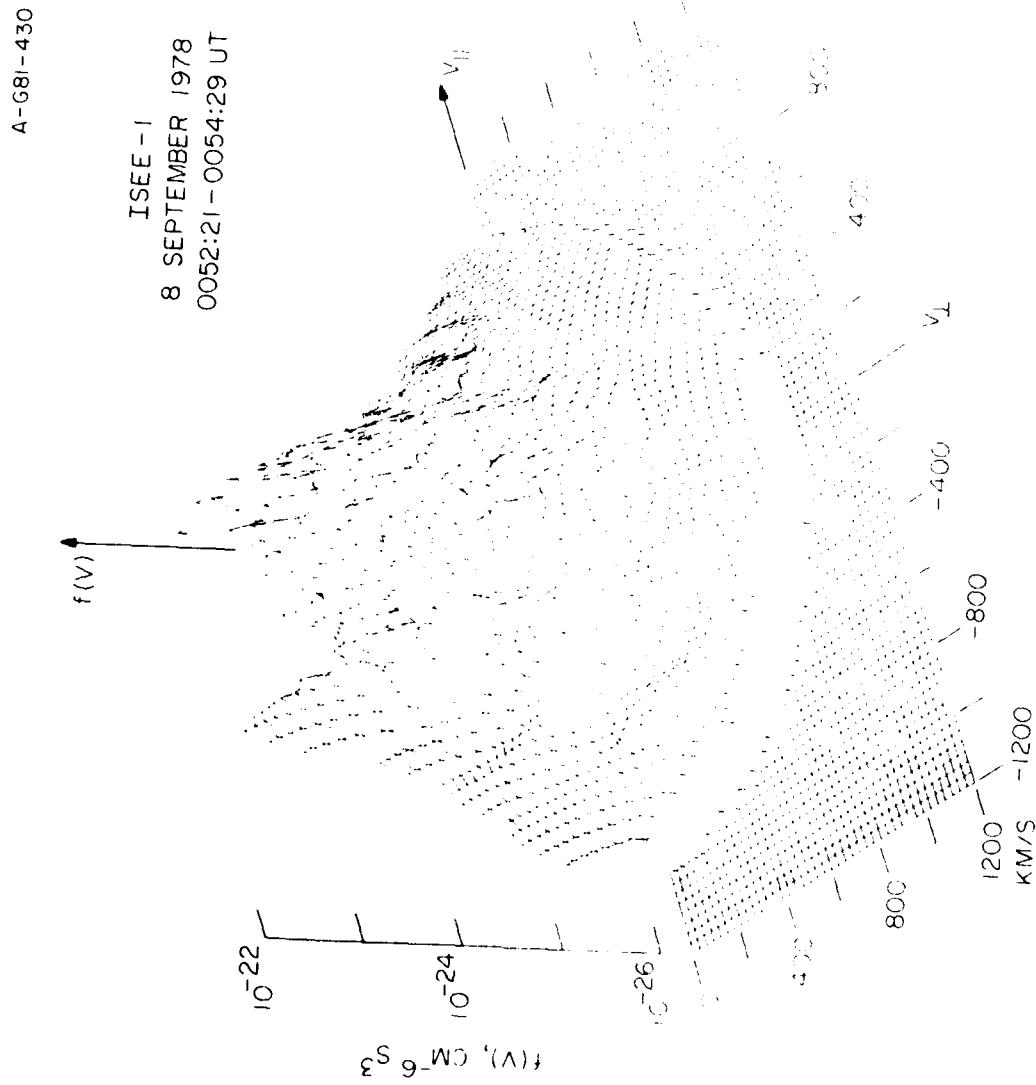
Figure 6

A-G8I-429

ISEE-1
8 SEPTEMBER 1978
0048:05-0050:13 UT

Figure 7

A-G8I-467
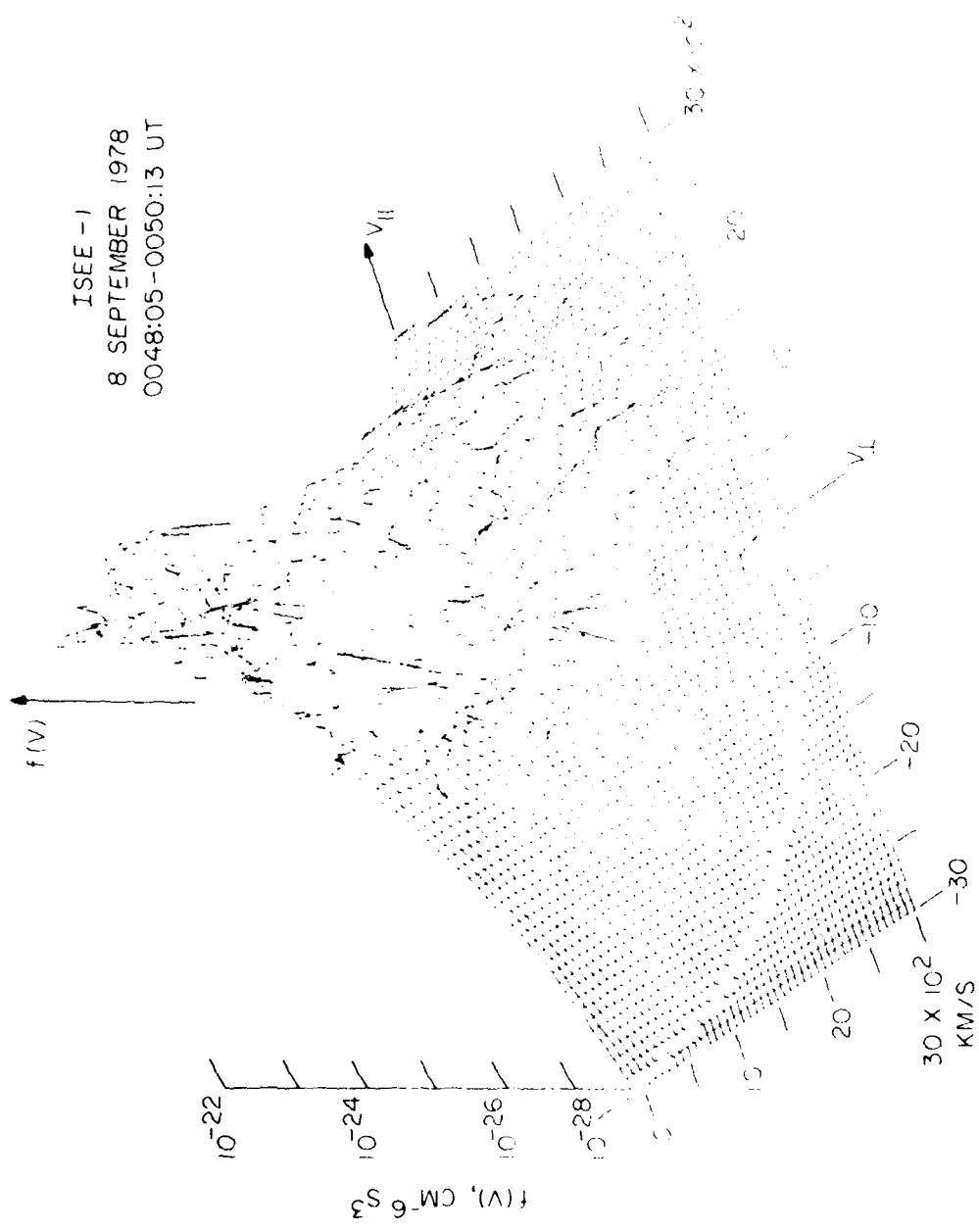
ISEE-I QUADRISPHERICAL LEPEDEA IONS
ISODENSITY CONTOURS OF DISTRIBUTION FUNCTION
8 SEPTEMBER 1978
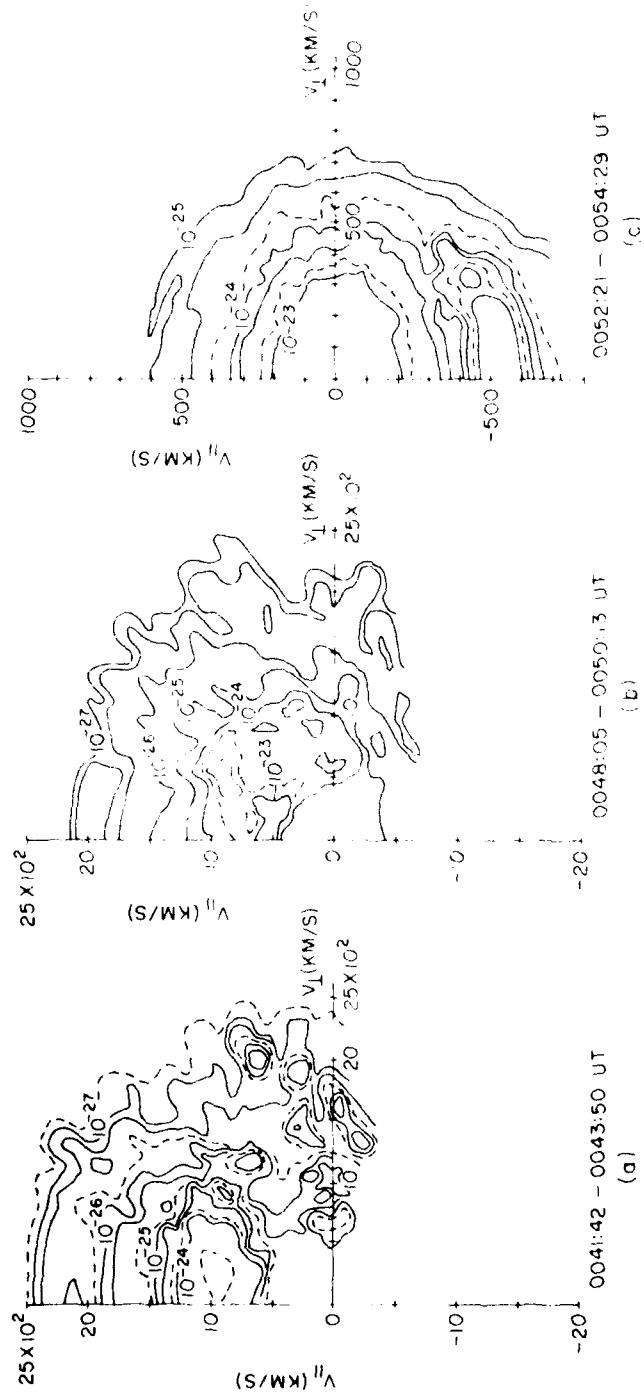
Figure 8

ENERGETIC ELECTRONS ($\geq$ 45 keV)

AVERAGE INTENSITIES AND ANGULAR DISTRIBUTIONS
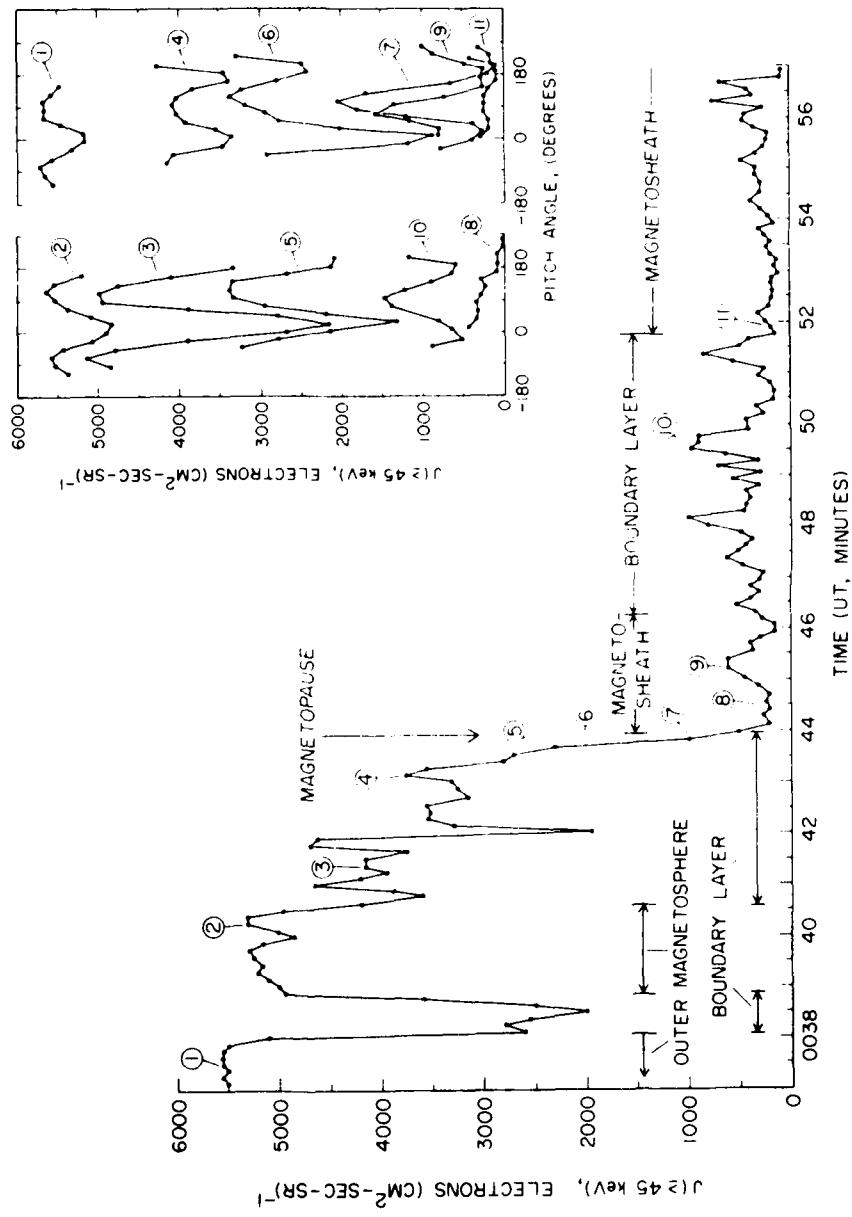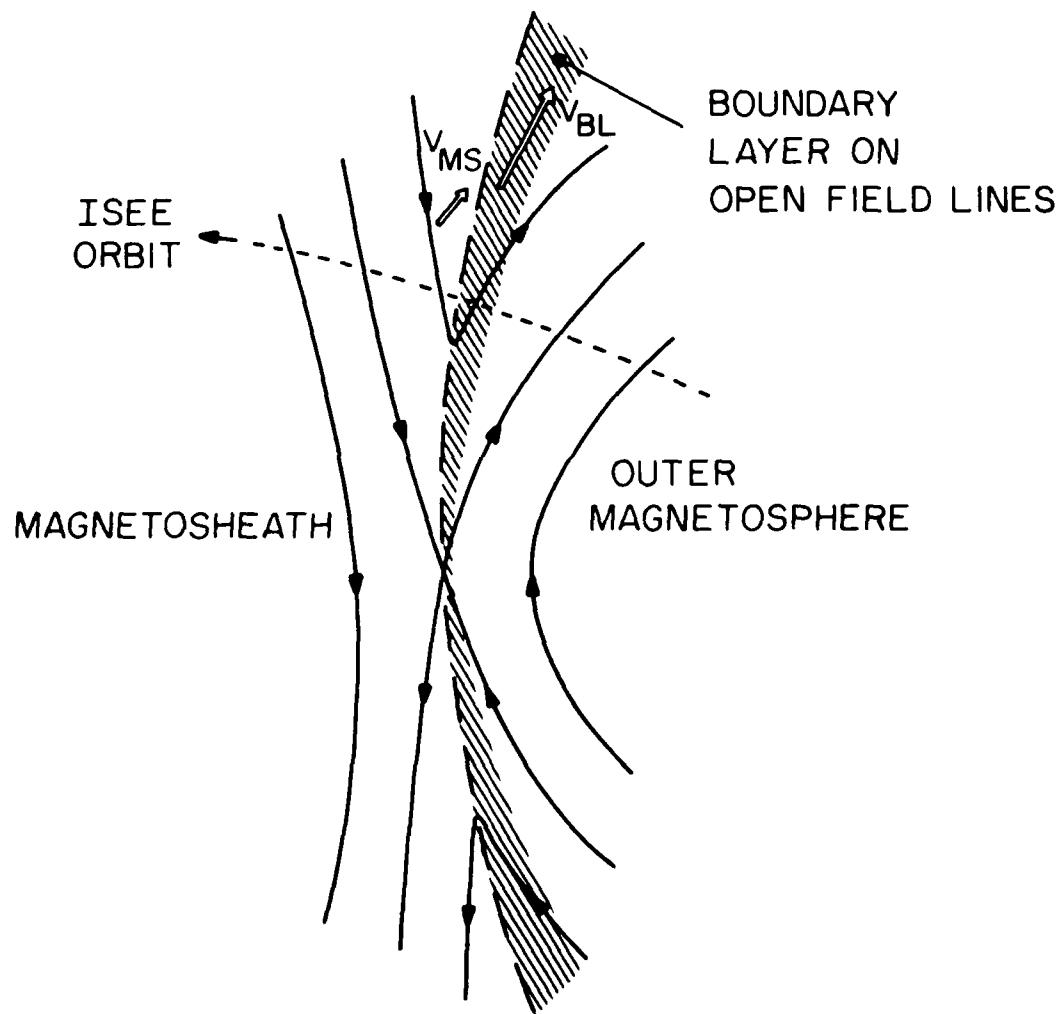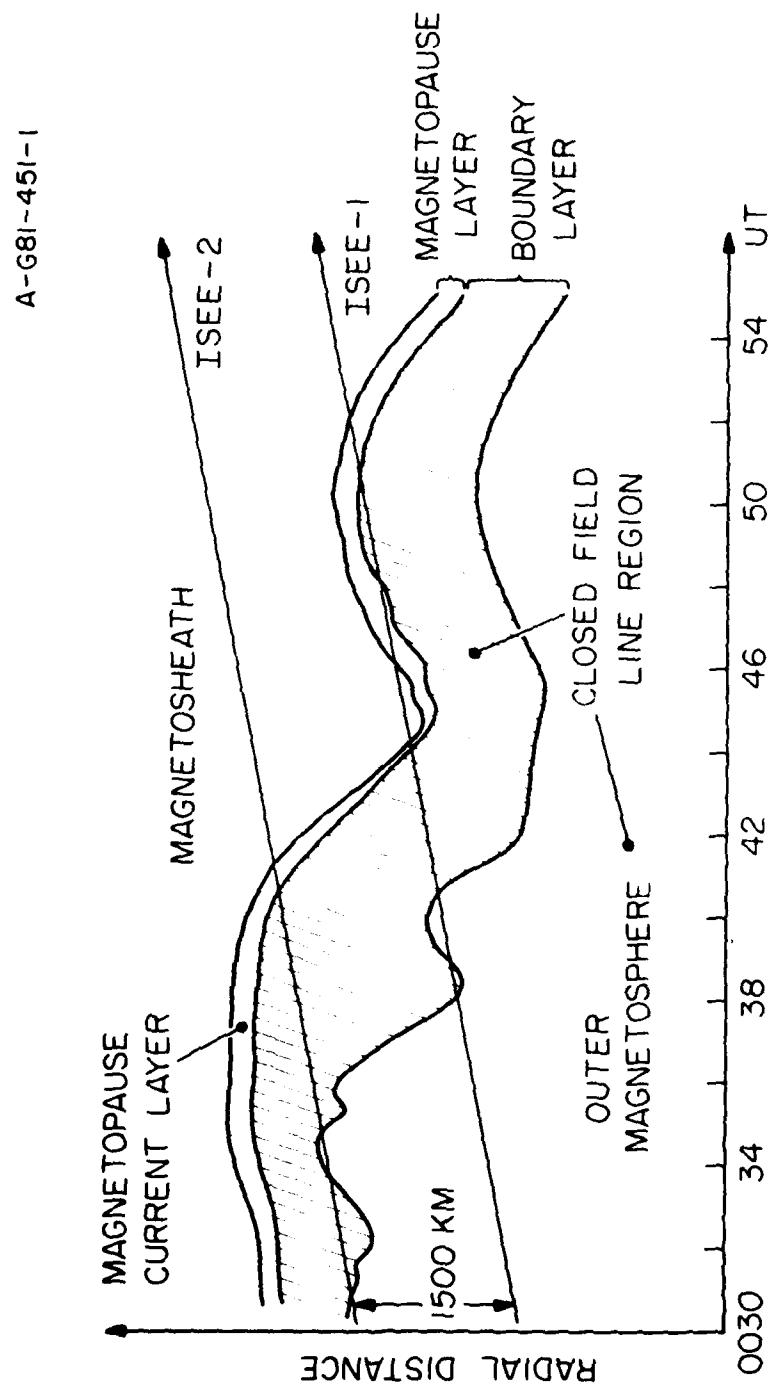
C-G81-289

Figure 9

A-G8l-452

ISEE
ORBIT

V_{MS}

V_{BL}

BOUNDARY
LAYER ON
OPEN FIELD LINES

MAGNETOSHEATH

OUTER
MAGNETOSPHERE

Figure 10

Figure 11

REPORT DOCUMENTATION PAGE		READ INSTRUCTIONS BEFORE COMPLETING FORM
1. REPORT NUMBER U of Iowa 81-16	2. GOVT ACCESSION NO. AD-A102 760	3. RECIPIENT'S CATALOG NUMBER -
4. TITLE (and Subtitle) Observations of High-Speed Plasma Flow Near the Earth's Magnetopause: Evidence for Reconnection?		5. TYPE OF REPORT & PERIOD COVERED Scientific - 1978
		6. PERFORMING ORG. REPORT NUMBER
7. AUTHOR(s) T. E. Eastman and L. A. Frank		8. CONTRACT OR GRANT NUMBER(s) N00014-76-C-0016
9. PERFORMING ORGANIZATION NAME AND ADDRESS Department of Physics and Astronomy The University of Iowa Iowa City, Iowa 52242		10. PROGRAM ELEMENT, PROJECT, TASK AREA & WORK UNIT NUMBERS
11. CONTROLLING OFFICE NAME AND ADDRESS Office of Naval Research Electronic and Solid State Sciences Program Arlington, Virginia 22217		12. REPORT DATE June 1981
		13. NUMBER OF PAGES 55
14. MONITORING AGENCY NAME & ADDRESS(if different from Controlling Office)		15. SECURITY CLASS. (of this report) UNCLASSIFIED
		15a. DECLASSIFICATION DOWNGRADING SCHEDULE

16. DISTRIBUTION STATEMENT (of this Report)

Approved for public release; distribution unlimited.

17. DISTRIBUTION STATEMENT (of the abstract entered in Block 20, if different from Report)

18. SUPPLEMENTARY NOTES

19. KEY WORDS (Continue on reverse side if necessary and identify by block number)

BOUNDARY LAYER
MAGNETOPAUSE
RECONNECTION

20. ABSTRACT (Continue on reverse side if necessary and identify by block number)

(see page following)

Abstract

In an attempt to confirm the evidence for reconnection reported by Paschmann et al. (1979) we have examined three-dimensional plasma velocity distributions sampled near the magnetopause using the LEPEDEA plasma instrument. During the magnetopause crossing of 8 September 1978, we observe high-speed plasma flow in the magnetospheric boundary layer which is suggestive of the accelerated flow predicted by reconnection models. However, simultaneous measurements of ≥ 45 keV energetic electrons show pancake-shaped pitch-angle distributions which indicate a closed field line regime whereas the high-speed plasma flow is predicted to occur on open field lines for the reconnection hypothesis. Low-energy plasma and energetic ion observations do not show any evidence for a local flow component normal to the magnetopause, and the energetic particle measurements show no evidence for a finite normal magnetic field component. Since the energetic particle angular distributions indicate that the high-speed plasma flow occurs partly or entirely on closed field lines, we suggest that the simplest hypothesis is to place the entire boundary layer observed during this crossing on closed field lines. We find that several detailed features of the available measurements can be explained readily in this way. Our ISEE observations appear to be most consistent with impulsive injection of magnetosheath plasma across the magnetopause in a process that involves both MHD and plasma kinetic instabilities.